International Journal on Magnetic Particle Imaging
Vol 3, No 1, Article ID 1703010, 7 Pages

Infinite Science Publishing

Research Article

Effects of Duty Cycle on Magnetostimulation Thresholds in MPI

Omer Burak Demirel[a,b,*] · Emine Ulku Saritas[a,b,c]

[a] Department of Electrical and Electronics Engineering, Bilkent University, Ankara, Turkey
[b] National Magnetic Resonance Research Center (UMRAM), Bilkent University, Ankara, Turkey
[c] Neuroscience Program, Aysel Sabuncu Brain Research Center, Bilkent University, Ankara, Turkey
[*] Corresponding author, email: demirel@ee.bilkent.edu.tr

Received 24 November 2016; Accepted 21 February 2017; Published online 23 March 2017

Abstract

Magnetic Particle Imaging (MPI) relies on time-varying magnetic fields to generate an image of the spatial distribution of superparamagnetic iron oxide nanoparticles. However, these oscillating magnetic fields form electric field patterns within the body, which in turn can cause peripheral nerve stimulations (PNS), also known as magnetostimulation. To prevent potential safety hazards and to optimize the scanning parameters such as field-of-view (FOV) and scanning speed in MPI, the factors that affect drive field magnetostimulation limits need to be determined accurately. In this work, we investigate the effects of the duty cycle on magnetostimulation thresholds in MPI. We performed human subject experiments by using a highly homogenous solenoidal coil on the upper arm of six subjects. Six different duty cycles ranging between 5 % and 100 % were applied at 25 kHz. Accordingly, magnetostimulation limits first decrease and then increase with increasing duty cycle, reaching a maximum at 100 % duty cycle. Since high duty cycles would be the preferred operating mode for rapid imaging with MPI, these results have promising implications for future human-sized MPI systems.

I. Introduction

Magnetic Particle Imaging (MPI) utilizes magnetic fields to image the distribution of superparamagnetic iron oxide nanoparticles with high spatial resolution and contrast [1–3]. The current applications of MPI include angiographic imaging [4, 5], cancer imaging [6], stem cell tracking [7, 8], temperature mapping [9], and combined imaging and hyperthermia [10, 11]. These imaging applications are made possible by time-varying magnetic fields that shift the position of the field-free point (FFP) in space, together with a strong static selection field (e.g., 3 T/m) that creates the FFP. Time-varying magnetic fields are subject to human safety limits on magnetostimulation (also called peripheral nerve stimulation) and specific absorption rate (SAR) [12–14]. Of these two factors, SAR limits were widely investigated for the radiofrequency (RF) fields in MRI (e.g., at 64 MHz or 128 MHz) [14]. Likewise, the magnetostimulation limits of MRI gradient fields operating at lower frequencies of around 1 kHz were also investigated, with the goal of achieving high resolution and rapid imaging capabilities [15, 16]. Similarly, the safety limits of the time-varying fields in MPI will also impact the imaging quality and speed.

Previous studies have shown that magnetostimulation is the main safety concern for drive field frequencies of up to 150 kHz [17–19]. One important result of these MPI human subject experiments was that the stimulation thresholds decrease with increasing frequency [17], and that the thresholds depend on the direction of the drive field [18–20]. Another result was that, independent of frequency, the magnetostimulation thresholds

decreased with increasing pulse duration, and stabilized for pulse durations longer than approximately 20 ms [21].

In this work, we investigate the effects of duty cycle on magnetostimulation thresholds for the drive field in MPI. We perform human subject experiments on six healthy subjects at six different duty cycles, ranging from 5 % to 100 % duty cycle at 25 kHz. We show that the magnetostimulation thresholds first decrease and then increase with increasing duty cycle, and that the stimulation thresholds at 100 % duty cycle are significantly higher than the ones at lower duty cycles. This result has promising implications, as operating at full-duty-cycle drive field would be desirable for rapid imaging purposes.

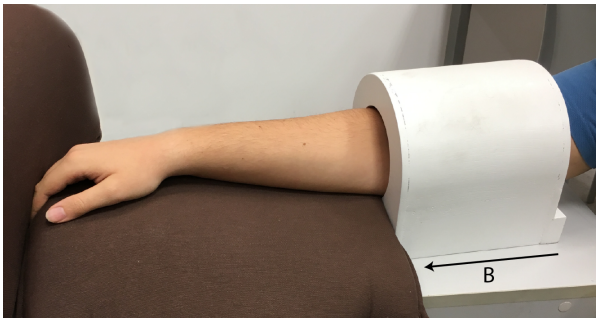

Figure 1: A solenodial coil was used to test magnetostimulation limits in the human upper arm with field homogeneity greater than 95 % in the axial direction in a 7 cm long region (magnetic field direction shown with an arrow).

II. Methods

We designed and conducted human subject experiments, approved by Bilkent University Ethics Committee. Our aim was to determine the relationship between duty cycle and magnetostimulation thresholds. All experiments were performed at a single frequency of 25 kHz, to determine the magnetic field amplitudes where the PNS sensations first become discernable. A total of six subjects were tested on the upper arm. The subjects described the magnetostimulation sensation as a twitching or tingling sensation at different intensities and at different locations on their arms. The subjects did not report any pain or discomfort during the study.

II.I. Magnetostimulation Setup

Magnetostimulation thresholds were tested with a solenoidal coil on the upper arm of the subjects (see Fig. 1). This solenoid had a bore size of 11 cm in diameter and 17 cm in length with greater than 95 % field homogeneity in a 7 cm long region, as previously described [17, 21]. The measured magnetic field amplitude was 410 μT/A at the center of the coil.

The amplitudes and duty cycles of the magnetic pulses were controlled via MATLAB, using a data acquisition module (NI USB-6363, National Instruments, Austin, TX) that sent the pulse shapes to the power amplifier (AE Techron 7224, AE Techron, Elkhart, IN). At the power limits of the amplifier, the maximum magnetic fields that could be generated varied from 72 mT-pp at 5 % duty cycle to 62 mT-pp at 100 % duty cycle. A Rogowski AC current probe (PEM, LFR 06/6/300, Nottingham, UK) was used to measure the current on the solenoid during each active interval. These measured current values were multiplied by the 410 μT/A sensitivity of the coil to record the magnetic field amplitudes. This procedure provided a real-time measurement of the magnetic field in the solenoid.

II.II. Adjusting Duty Cycle

For testing duty cycle dependence, the experiments required the following conditions: (1) the subject must have enough time to report a magnetostimulation sensation, (2) the sensations must be sufficiently isolated in time to avoid interference between neighboring repetition times, (3) the experiment must allow testing a wide range of duty cycles, and (4) the entire experiment must fit within 20–30 minutes to keep the subject engaged. The first two conditions necessitated the use of an idle period to give the subjects time to report stimulation sensations and to enable them to distinguish each repetition period. The third condition required the active interval for applying magnetic pulses to be as long as possible, while the fourth condition required the overall repetition time to be as short as possible.

An initial test on a single subject was performed to determine the overall repetition time. During this test, we applied 100 ms duration pulses at 2 s, 3 s, and 4 s repetition times. Subject responses showed less than 1 % variation among these three repetition times (results not shown). Hence, considering all four conditions listed above, an overall repetition time of 4 s was chosen, where the magnetic pulses were applied during the first 2 s (active interval, T_{active}), followed by an idle 2 s resting interval to allow the subject to report stimulation and for the nerves to rest. For determining the duty cycle, we have taken T_{active} as reference. Hence, a continuous magnetic pulse applied throughout T_{active} corresponded to a 100 % duty cycle case.

Next, since earlier experiments on the duration dependence of magnetostimulation limits revealed that the thresholds stabilize for pulses longer than 20 ms [21], a pulse duration of $T_{\text{pulse}} = 100$ ms was chosen in this work (see Fig. 2(a)). The experiment was designed to include six different duty cycles (5 %, 10 %, 25 %, 50 %, 75 %, and 100 %) at 25 kHz. Duty cycle, D, was defined as follows:

$$D = \frac{N_{\text{pulse}} \times T_{\text{pulse}}}{T_{\text{active}}} \times 100 \qquad (1)$$

10.18416/ijmpi.2017.1703010

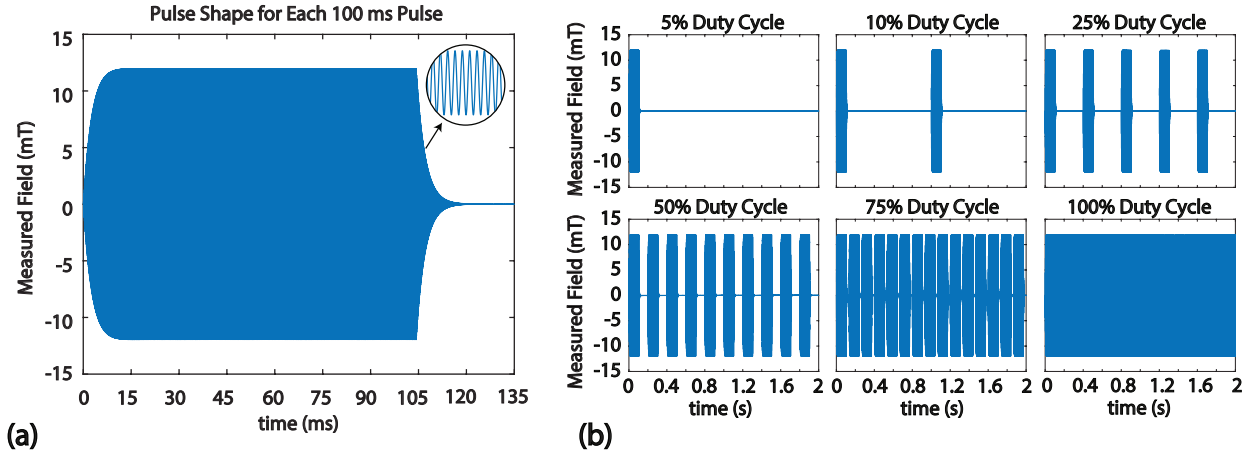

Figure 2: Six different duty cycles were tested at 25 kHz. (a) Due to inductive/capacitive effects of the experimental setup, each measured pulse of 100 ms duration displayed non-zero ramp up/down times. (b) The measured fields for the duty cycles used in this work: 5 %, 10 %, 25 %, 50 %, 75 %, and 100 % duty cycles. The duration of the active interval was 2 s.

where N_{pulse} is the number of equidistant, equal-amplitude 100 ms pulses applied during an active interval (see Fig. 2(b)). In the 100 % duty cycle case, a continuous pulse was applied during the entire active interval.

Due to the inductive/capacitive effects in the experimental setup, we observed non-zero ramp up and ramp down times (see Fig. 2(a)). Here, we did not aim to reduce these ramp up/down times, as they were less than 15 ms in duration. The remaining 70 ms of the pulse had a flat envelope, safely overcoming any pulse duration effect that may stem from utilizing short pulses [21]. Here, we calculated the resulting duty cycles directly from the measured magnetic fields [22]:

$$D_{\text{meas}} = \left[\frac{P_{\text{meas}}}{P_{100\%}}\right] \times 100 \tag{2}$$

$$= \left[\frac{B_{\text{RMS}}}{B_{\text{peak}}/\sqrt{2}}\right]^2 \times 100 \tag{3}$$

$$= \left[\frac{1}{T_{\text{active}}} \int_0^{T_{\text{active}}} B^2_{\text{meas}}(t)\,dt\right] \frac{2}{\max^2(B_{\text{meas}})} \times 100\,. \tag{4}$$

These calculations are valid for the case of a flat-envelope sinusoidal drive field, as utilized in this work. Here, RMS refers to the root-mean-squared value of the measured magnetic field, calculated via integrating over the entire T_{active} period. Accordingly, we found 5.1 %, 10.2 %, 25.4 %, 50.8 %, 76.4 %, and 99.8 % for the duty cycles, indicating a close match to the targeted values.

II.III. Human Subject Experiments

A total of six healthy male subjects were recruited, after screening for safety considerations (i.e., metallic implants, metal objects, pacemakers, etc.). The mean and standard deviations for the age, weight, and height of the subjects were 26 ± 3 years, 86 ± 12 kg, and 181 ± 5 cm. Each subject was tested 3 times on different days, with a total of 18 experiments conducted. Each experiment lasted approximately 25–30 minutes. Subjects were in a seating position with their upper arms inside the solenoidal coil, wearing an over-the-head earmuff to help them concentrate on the experiment. They were instructed to click a mouse button whenever they felt a stimulation sensation.

The order in which the duty cycles were tested was randomized at the beginning of each experiment. The first part of the test for each duty cycle started from a low magnetic field amplitude. Then, the field amplitude was slowly increased to determine an approximate threshold level, B_{center}, from the subject's responses. Next, a secondary test was performed to more accurately determine the threshold level. The field amplitudes in this secondary test were chosen in random order to avoid any biasing and hysteresis effect [17]. Here, the field amplitudes were randomized in the ±15 % range of B_{center} with a step size of 1 % of B_{center}. For each repetition time, the response of the subject was recorded together with the measured field amplitude. A numeric value of "1" was assigned to stimulation response (as reported by the subject via a mouse click), and a numeric value of "0" was assigned if the subject remained unresponsive (see Fig. 3). This two-step procedure was repeated at each duty cycle. At the end of the experiment, the subject was asked to describe the stimulation sensation and report the approximate stimulation location on their arm.

II.IV. Data Analysis

Similar to our previous studies [17, 21], we modeled the magnetostimulation threshold as a probabilistic param-

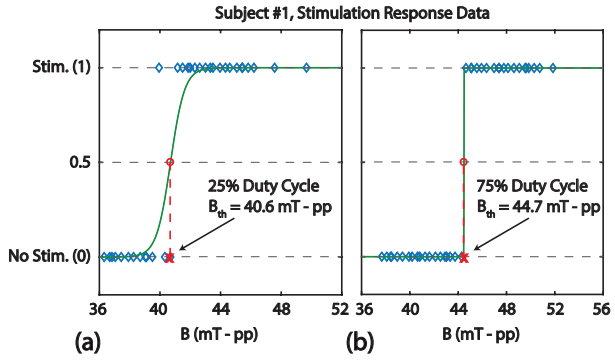

Figure 3: Stimulation response data for Subject #1 for 25 % and 75 % duty cycles at 25 kHz. Blue diamonds represents the subject's responses: "1" denotes that the subject felt a stimulation sensation and "0" denotes that the subject did not experience stimulation. The green curves represent fitted sigmoid functions, and red circles denote the estimated threshold levels. (a) Soft transition ($W = 0.23$ mT-pp) with $B_{\text{th}} = 40.6$ mT-pp at 25 % duty cycle. (b) Sharp transition ($W = 0.0023$ mT-pp) with $B_{\text{th}} = 44.7$ mT-pp at 75 % duty cycle. In these example data sets, subject's threshold level increased from 40.6 mT-pp at 25 % duty cycle to 44.7 mT-pp at 75 % duty cycle.

eter to allow for inconsistencies in subject responses. Accordingly, we used a cumulative distribution function (CDF) given by a sigmoid curve:

$$F(B) = \left(1 + e^{\frac{-(B-B_{\text{th}})}{W}}\right)^{-1}. \tag{5}$$

Here, B (mT-pp) is the peak-to-peak magnetic field strength, B_{th} (mT-pp) is the 50 % crossing of the sigmoid curve (i.e., the determined stimulation threshold), and W (mT-pp) is the transition width with smaller W representing sharper transitions. At each duty cycle, the subject's responses were fitted to this sigmoid curve via a Levenberg-Marquardt nonlinear least-squares regression, to yield B_{th} and W. Example stimulation-response data are shown in Fig. 3 for Subject #1 at two different duty cycles. Fig. 3(a) shows a soft transition case at 25 % duty cycle with $W = 0.23$ mT-pp due to a few inconsistent responses from the subject. On the other hand, Fig. 3(b) shows a sharp transition case at 75 % duty cycle with $W = 0.0023$ mT-pp, without any inconsistent responses.

For statistical analysis purposes, the data from each experiment was first normalized by the mean threshold within that experiment. Next, the normalized curves from all 3 experiments for a subject were averaged. This procedure was repeated for all subjects. Finally, a paired Wilcoxon signed rank test was performed to test whether the subjects' responses were significantly different at different duty cycles.

III. Results

Fig. 4(a) shows the magnestostimulation thresholds as a function of duty cycle for a single subject (Subject #1), for three repetition experiments performed on different days. While the overall trend remains the same, the magnetostimulation thresholds show slight variations among the three repetitions, potentially due to differences in the positioning of the subject's arm within the coil. To better observe the overall trend, we normalized the data from each experiment by the mean magnetostimulation threshold within the corresponding experiment. The normalized curves plotted in Fig. 4(b) show that the magnetostimulation thresholds first decrease and then increase with increasing duty cycle. In all three experiments, the 100 % duty-cycle cases display the highest stimulation thresholds.

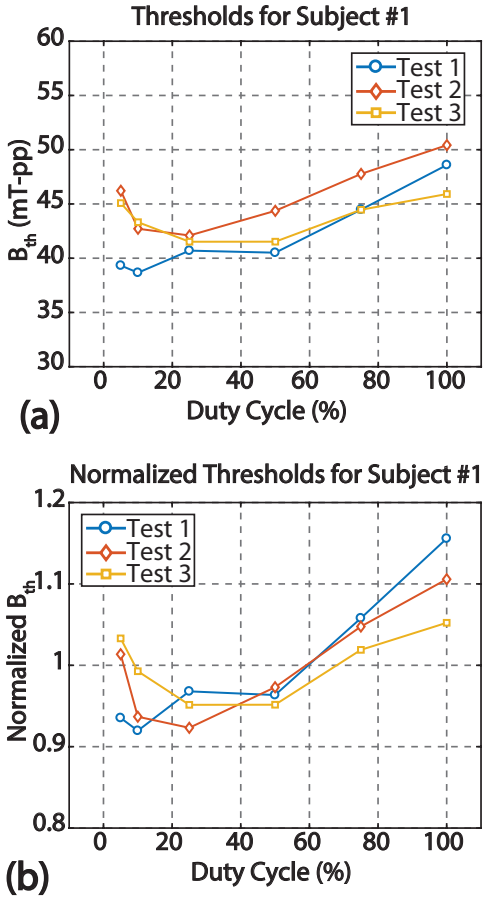

Figure 4: (a) Magnetostimulation threshold as a function of duty cycle for three different experiments on Subject #1. (b) Magnetostimulation thresholds normalized by the mean threshold value for each experiment. In all three experiments, the highest threshold levels were reached at 100 % duty cycle.

Fig. 5 displays the normalized magnetostimulation thresholds for all subjects ($N = 6$) using all 18 experiments. The plotted curve shows the mean thresholds

of all 6 subjects and the error bars denote the standard errors to reflect intersubject variations. Accordingly, the magnetostimulation thresholds first decrease and then increase with increasing duty cycle, reaching a peak value at 100 % duty cycle. The thresholds at 100 % duty cycle are approximately 6 % higher than those at 5 % duty cycle, and approximately 8 % higher than those at the 10 % to 75 % duty cycles. Our statistical analysis also showed that the thresholds at 100 % duty cycle were significantly higher than those at lower duty cycles ($p < 0.031$, paired Wilcoxon signed rank test). In addition, the thresholds at 5 % duty cycle were significantly higher than those at 10 % duty cycle ($p < 0.031$, paired Wilcoxon signed rank test). There were no statistically significant differences among other duty cycles.

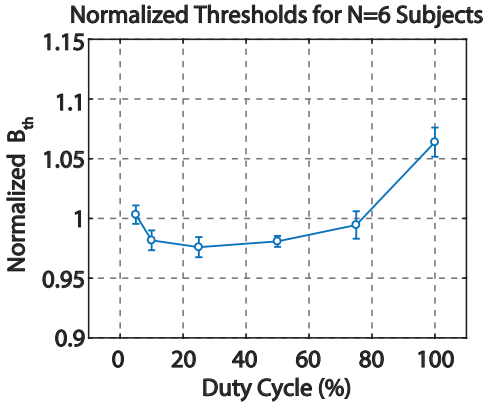

Figure 5: Normalized magnetostimulation thresholds as a function of duty cycle for all subjects ($N = 6$), using all 18 experiments. The curve gives the mean thresholds and the error bars denote the standard errors to reflect intersubject variations. Magnetostimulation limits first decrease with increasing duty cycle, and then increase to reach a peak value at 100 % duty cycle.

IV. Discussion

This work investigated the effects of duty cycle on magnetostimulation thresholds for the drive field in MPI at 25 kHz. The human-subject experiments revealed that threshold levels first decrease with increasing duty cycle, then increase again and reach a maximum at 100 % duty cycle. Accordingly, this full-duty-cycle case yielded up to 8 % higher thresholds than at lower duty cycles. These results suggest that the effect of duty cycle on magnetostimulation thresholds is relatively small when compared to the effects of frequency [17] or pulse duration [21]. Having only a small variation in thresholds at different duty cycles is a promising result in itself, since different imaging applications may require the usage of different duty cycles. Having higher thresholds for the full duty cycle case is a further encouraging result, as it is desirable to operate at 100 % duty cycle to minimize the total scan time, e.g., by using a continuous drive field together with a focus field that covers a wide imaging FOV [23].

In the literature, there has been numerous studies on finding the optimum duty cycle for electrical stimulation used for the purposes of muscle rehabilitation and pain control [24–26]. These studies looked at muscle torque production by using alternating currents from 0.5 kHz to 20 kHz, and unanimously observed that the stimulation efficiency was the highest at approximately 20 % duty cycle. Interestingly, these studies were conducted under very different conditions than ours. First, an electrical stimulation was utilized instead of magnetic stimulation. More importantly, the duration between bursts was set to 50 Hz (i.e., 20 ms interval), and the burst duration was varied. Despite these major differences, their findings are consistent with the results of our work, as we observed that 25 % duty cycle had the lowest magnetostimulation thresholds (the closest to 20 % duty cycle among the values that we tested). According to these electrical stimulation studies, the threshold for nerve excitation decreases with multiple bursts of pulses or with prolonged burst durations, which explains the initial decline in the threshold vs. duty cycle curve. However, extended durations or bursts may eventually decrease the response of the nerves due to synaptic fatigue from repetitive action potentials [25]. In fact, during our human-subject experiments, we visually observed that the muscles at the location of magnetostimulation remained contracted throughout the entire 2 s pulse duration for the 100 % duty cycle case, which could cause tiredness or numbness in the nerves.

In this work, the 5 % duty-cycle case corresponded to a single pulse with 100 ms pulse duration, and the 100 % duty-cycle case corresponded to a single pulse with 2 s pulse duration (see Fig. 2(b)). Our previous work on the relationship between pulse duration and magnetostimulation thresholds showed that, independent of operating frequency, the threshold levels were stabilized for pulses longer than 20 ms [21]. Hence, one would expect the 5 % and 100 % duty cycle cases to yield the same magnetostimulation thresholds. Interestingly, this was not the case in our results, as 100 % duty cycle showed approximately 6 % higher thresholds. One potential explanation for this discrepancy is that our previous work investigated pulse durations of up to 125 ms and not further.

During our preliminary experiments, we conducted experiments on both the lower arms and upper arms of the subjects. Except for a few subjects, the power amplifier used in this work did not have sufficient power to induce magnetostimulation on the lower arm (results not shown). On the other hand, the same subjects experienced magnetostimulation at the same magnetic field levels when tested on their upper arms. This result is consistent with our previous work, which showed

that magnetostimulation limits decrease with increasing body part size [17]. While the upper arm proved to be an easier location for inducing stimulation, the limits of the power amplifier prohibited us from recruiting female subjects, whose upper arms are relatively smaller in diameter. However, we do not expect there to be any gender differences in the duty-cycle effects described in this work, except for the global scaling of the absolute magnetostimulation limits.

Current MPI scanners utilize drive field frequencies in the range of 10 kHz to 150 kHz [27]. Here, we investigated the effects of duty cycle on magnetostimulation thresholds at 25 kHz only. Our previous work on pulse-duration-dependence of nerve stimulations showed that the trends remained the same, independent of operating frequency [21]. Accordingly, we expect the trends for duty cycle dependence to also remain the same at different operating frequencies, which remains to be shown experimentally.

V. Conclusion

In this work, we showed with human-subject experiments that the magnetostimulation thresholds first decrease and then increase with increasing duty cycle, reaching a peak value at 100 % duty cycle. These results have promising consequences for rapid imaging in MPI, since operating at full duty cycle would be the preferred mode for most imaging applications.

Acknowledgments

The authors would like thank Mustafa Can Delikanlı for his assistance with the experimental setup. This work was supported by the European Commission through an FP7 Marie Curie Career Integration Grant (PCIG13-GA-2013-618834), and by the Turkish Academy of Sciences through TUBA-GEBIP 2015 program, and by the Science Academy through BAGEP 2016 award.

References

[1] B. Gleich and J. Weizenecker. Tomographic imaging using the nonlinear response of magnetic particles. *Nature*, 435(7046):1214–1217, 2005. doi:10.1038/nature03808.

[2] E. U. Saritas, P. W. Goodwill, L. R. Croft, J. J. Konkle, K. Lu, B. Zheng, and S. M. Conolly. Magnetic Particle Imaging MPI for NMR and MRI researchers. *J. Magn. Reson.*, 229:116–126, 2013. doi:10.1016/j.jmr.2012.11.029.

[3] T. M. Buzug. From Magnetic Nanoparticle Spectroscopy to Imaging Methodology. *Intern. J. Magnetic Particle Imaging*, 2(1): 1610000, 2016. doi:10.18416/ijmpi.2016.1610000.

[4] J. Weizenecker, B. Gleich, J. Rahmer, H. Dahnke, and J. Borgert. Three-dimensional real-time in vivo magnetic particle imaging. *Phys. Med. Biol.*, 54(5):L1–L10, 2009. doi:10.1088/0031-9155/54/5/L01.

[5] K. Lu, P. W. Goodwill, E. U. Saritas, B. Zheng, and S. M. Conolly. Linearity and Shift Invariance for Quantitative Magnetic Particle Imaging. *IEEE Trans. Med. Imag.*, 32(9):1565–1575, 2013. doi:10.1109/TMI.2013.2257177.

[6] E. Yu, M. Bishop, P. W. Goodwill, B. Zheng, M. Ferguson, K. M. Krishnan, and S. M. Conolly. First Murine in vivo Cancer Imaging with MPI. In *International Workshop on Magnetic Particle Imaging*, 2016.

[7] B. Zheng, T. Vazin, P. W. Goodwill, A. Conway, A. Verma, E. U. Saritas, D. Schaffer, and S. M. Conolly. Magnetic Particle Imaging tracks the long-term fate of in vivo neural cell implants with high image contrast. *Sci. Rep.*, 5:14055, 2015. doi:10.1038/srep14055.

[8] K. Them, J. Salamon, P. Szwargulski, S. Sequeira, M. G. Kaul, C. Lange, H. Ittrich, and T. Knopp. Increasing the sensitivity for stem cell monitoring in system-function based magnetic particle imaging. *Phys. Med. Biol.*, 61(9):3279–3290, 2016. doi:10.1088/0031-9155/61/9/3279.

[9] C. Stehning, B. Gleich, and J. Rahmer. Simultaneous magnetic particle imaging (MPI) and temperature mapping using multicolor MPI. *Intern. J. Magnetic Particle Imaging*, 2(2):1612001, 2016. doi:10.18416/ijmpi.2016.1612001.

[10] K. Murase, M. Aoki, N. Banura, K. Nishimoto, A. Mimura, T. Kuboyabu, and I. Yabata. Usefulness of Magnetic Particle Imaging for Predicting the Therapeutic Effect of Magnetic Hyperthermia. *Open Journal of Medical Imaging*, 5(2):85–99, 2015. doi:10.4236/ojmi.2015.52013.

[11] D. Hensley, P. W. Goodwill, R. Dhavalikar, Z. W. Tay, B. Zheng, C. Rinaldi, and S. M. Conolly. Imaging and Localized Nanoparticle Heating with MPI. In *International Workshop on Magnetic Particle Imaging*, 2016.

[12] J. P. Reilly. Peripheral nerve stimulation by induced electric currents: Exposure to time-varying magnetic fields. *Med. Biol. Eng. Comput.*, 27(2):101–110, 1989. doi:10.1007/BF02446217.

[13] J. P. Reilly. Maximum pulsed electromagnetic field limits based on peripheral nerve stimulation: application to IEEE/ANSI C95.1 electromagnetic field standards. *IEEE Trans. Biomed. Eng.*, 45(1): 137–141, 1998. doi:10.1109/10.650371.

[14] P. A. Bottomley and W. A. Edelstein. Power deposition in whole-body NMR imaging. *Med. Phys.*, 8(4):510–512, 1981. doi:10.1118/1.595000.

[15] F. Schmitt, W. Irnich, and H. Fischer. *Physiological Side Effects of Fast Gradient Switching*, pages 201–252. Springer, Berlin/Heidelberg, 1998. doi:10.1007/978-3-642-80443-4_7.

[16] W. Irnich and F. Schmitt. Magnetostimulation in MRI. *Magn. Reson. Med.*, 33(5):619–623, 1995. doi:10.1002/mrm.1910330506.

[17] E. U. Saritas, P. W. Goodwill, G. Z. Zhang, and S. M. Conolly. Magnetostimulation Limits in Magnetic Particle Imaging. *IEEE Trans. Med. Imag.*, 32(9):1600–1610, 2013. doi:10.1109/TMI.2013.2260764.

[18] I. Schmale, B. Gleich, J. Schmidt, J. Rahmer, C. Bontus, R. Eckart, B. David, M. Heinrich, O. Mende, O. Woywode, J. Jokram, and J. Borgert. Human PNS and SAR study in the frequency range from 24 to 162 kHz. In *International Workshop on Magnetic Particle Imaging*, 2013. doi:10.1109/IWMPI.2013.6528346.

[19] I. Schmale, B. Gleich, J. Rahmer, C. Bontus, J. Schmidt, and J. Borgert. MPI Safety in the View of MRI Safety Standards. *IEEE Trans. Magn.*, 51(2):6502604, 2015. doi:10.1109/TMAG.2014.2322940.

[20] E. Yu, E. U. Saritas, and S. M. Conolly. Comparison of magnetostimulation limits for axial and transverse drive fields in MPI. In *International Workshop on Magnetic Particle Imaging*, 2013. doi:10.1109/IWMPI.2013.6528324.

[21] E. U. Saritas, P. W. Goodwill, and S. M. Conolly. Effects of pulse duration on magnetostimulation thresholds. *Med. Phys.*, 42(6): 3005–3012, 2015. doi:10.1118/1.4921209.

[22] M. I. Skolnik. *Introduction to Radar Systems*. McGraw-Hill Book Company, Singapore, 1962.

[23] O. B. Demirel, D. Sarica, and E. U. Saritas. Rapid Scanning in X-Space MPI: Impacts on Image Quality. In *International Workshop*

on Magnetic Particle Imaging, 2016.

[24] J. Moreno-Aranda and A. Seireg. Investigation of over-the-skin electrical stimulation parameters for different normal muscles and subjects. *J. Biomech.*, 14(9):587–593, 1981. doi:10.1016/0021-9290(81)90084-1.

[25] A. R. Ward, V. J. Robertson, and H. Ioannou. The effect of duty cycle and frequency on muscle torque production using kilohertz frequency range alternating current. *Med. Eng. Phys.*, 26(7):569–579, 2004. doi:10.1016/j.medengphy.2004.04.007.

[26] R. E. Liebano, S. Waszczuk Jr., and J. B. Corrêa. The Effect of Burst-Duty-Cycle Parameters of Medium-Frequency Alternating Current on Maximum Electrically Induced Torque of the Quadriceps Femoris, Discomfort, and Tolerated Current Amplitude in Professional Soccer Players. *J. Orthop. Sports Phys. Ther.*, 43(12):920–926, 2013. doi:10.2519/jospt.2013.4656.

[27] N. Panagiotopoulos, R. L. Duschka, M. Ahlborg, G. Bringout, C. Debbeler, M. Graeser, C. Kaethner, K. Lüdtke-Buzug, H. Medimagh, J. Stelzner, T. M. Buzug, J. Barkhausen, F. M. Vogt, and J. Haegele. Magnetic particle imaging: current developments and future directions. *Int. Journ. Nanomed.*, 10:3097, 2015. doi:10.2147/IJN.S70488.

